JOURNAL OF APPLIED ELECTROCHEMISTRY 17 (1987) 283–293

*The corrosion and deposition performance of molten salt electrodeposited chromium coatings**

A. M. EMSLEY, M. P. HILL

Central Electricity Research Laboratories, Technology Planning and Research Division of the Central Electricity Generating Board, Leatherhead, Surrey KT22 7SE, UK

Received 10 April 1986

Chromium coatings have been prepared by electrodeposition from a LiCl–KCl eutectic at 450° C, using a potential pulse method to control the nucleation stage of deposition prior to the main growth. Pure crystalline chromium layers, 30 μm thick, were formed that were both coherent and adherent. The possible application of these coatings to nuclear reactor fuel cladding (20% chromium/25% nickel, niobium-stabilized stainless steel) to protect against carbon deposition and oxidation has been investigated.

In methane atmospheres at ~ 800° C the coatings are highly effective at reducing carbon pick-up, e.g. by a factor of 11 times after 640 h exposure. The protection mechanism is discussed. In high-temperature oxidation tests in CO_2-based atmospheres, the coatings do not confer protection. At 950° C there is severe spalling and at 860° C the oxidation rate is 2 to 3 times greater than that of an untreated control. The hardness of the chromium layer is low (150–270 kg mm^{-2}) compared to most other types of chromium coating. The use of carburization to increase the hardness has been investigated. Factors influencing the optimum coating thickness on this steel to achieve a satisfactory lifetime are discussed.

1. Introduction

The possible use of chromium protective coatings arises from a study of the mechanism of carbon deposition reactions from CO and CH_4 on the fuel cladding alloy of the advanced gas-cooled reactor (AGR). Carbon deposition could have various consequences, in particular an impairment of heat transfer. It has been shown that the chromium present in the alloy suppresses deposition by reducing the activity of the most important catalyst in the steel, i.e. iron [1]. To improve the carbon deposition performance without influencing the bulk metallurgical properties suggests the use of a coating. Experiments with pack-diffusion chromium coatings confirmed that good protection was conferred, this type of coating being strongly adherent [2]. Some of the disadvantages of this technique are the incorporation of the alumina–kaolin pack materials into the coating, and the high processing temperature (1050° C) that can cause unacceptable changes in the metallurgical properties of the fuel can alloy.

Another high-temperature diffusion coating technique is metalliding [3]. Chromium coatings can be electrodeposited and form a diffusion bonded layer in one step at $T \sim 950°$ C using a molten fluoride bath [4]. However, in the published method [4] the process was not adequately controlled electrochemically.

In order to define the coating parameters the electrodeposition of chromium layers at 450° C from chloride melts has been studied, and has led to the specification of a new coating process [5]. In addition to suppressing localized carbon deposition the coating must have sufficient corrosion resistance to withstand the CO_2 reactor coolant at temperatures up to ~ 850° C. The oxide layer which forms on the uncoated steel

* This paper was presented at a workshop on the electrodeposition of refractory metals, held at Imperial College, London, in July 1985.

0021-891X/87 $03.00 + .12

Table 1. Conditions for chromium electrodeposition

	Cr^{2+} conc. ($mol\,dm^{-3}$)	Initial nucleation pulse overpotential (mV)	Number of pulses	Deposition overpotential (mV)
1	0.77	−1100	2	−710
2	1.0	−600	3	−50
3	1.61	−600	1	−50

$T = 450°$ C; LiCl–KCl eutectic; coating thickness = 30 μm.

can spall leading to enhanced oxidation. A protective chromium layer might appear to help, but at high temperatures pure chromium sesquioxide can spall more rapidly than the iron–nickel–chromium mixed spinel oxide normally formed on the steel. It has been necessary to evaluate fully the coatings in CO_2-based atmospheres close to the peak local random operating temperatures of the reactor fuel cladding and well above, i.e. at temperatures between 850° C and 950° C.

2. Experimental details

2.1. *Coating treatment*

The coating conditions applicable to the AGR fuel cladding specimens used in these tests are given in Table 1. Details of the process have been given elsewhere [5, 6]. The deposition overpotentials were measured with respect to a Ag–AgCl 0.5 M reference electrode. Coated specimens were rinsed in water to remove remaining salts, washed in acetone and dried in air. A coating thickness of 30 μm was selected because previous work in this laboratory with pack-diffusion coatings had indicated that this was required to achieve a minimum lifetime of 2 years in an oxidizing environment.

The coated surface had a matt granular appearance (Fig. 1a). The fuel cladding, with its ribs designed to improve heat transfer, is covered uniformly over the rib tops, sides and in the rib roots as shown in the damaged area (Fig. 1b). The deposit is crystalline with an average crystal size of 10–30 μm at the outer surface (Fig. 1c).

2.2. *Evaluation tests*

The corrosion and deposition experiments were carried out in glass-lined pressure balanced autoclaves described previously [7]. The full test conditions are given in Table 2.

The methane for the deposition tests was dried and higher hydrocarbons removed in beds of 5A and 13X molecular sieve. The reaction conditions chosen give severe deposition compared to that in the AGR, but rapidly produce a catalytically grown carbon with an identical morphology to that observed in reactor grown deposits.

Oxidation tests were carried out at high pressures in a simulated AGR gas consisting of CO_2 with additions of 1.0% CO + 300 p.p.m. (vol.) CH_4 + 250 p.p.m. (vol.) H_2O + 100 p.p.m. (vol.) H_2. A low pressure test in pure CO_2 was carried out on specimens produced early in the programme. In both types of test, specimens were

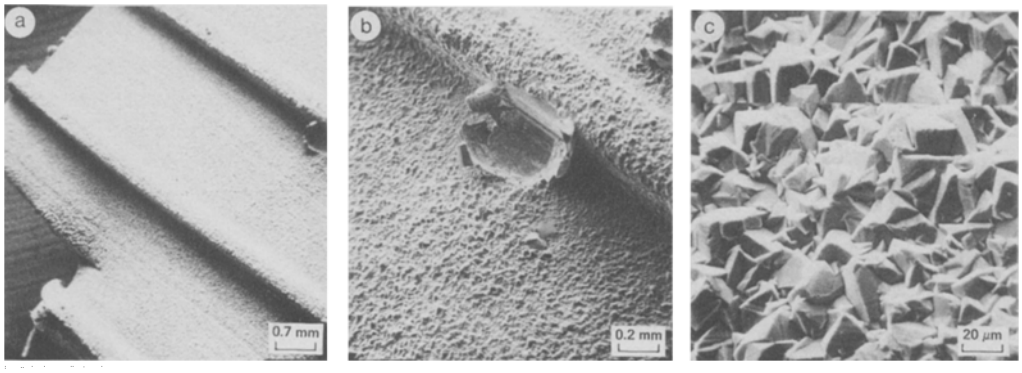

Fig. 1. Chromium-coated 20/25 niobium steel, as-prepared, showing (a) uniform coverage over the 375 μm square section ribs; (b) good throwing power in the rib root; (c) crystalline nature of the coating.

Table 2. Coating evaluation tests

Coating conditions (see Table 1)	*Pre-treatment*	*Test*	*Temperature (° C)*	*Gas*	*Pressure (Pa × 10^5)*
1	1100° C anneal for 50 h	Deposition	800/810	CH_4	1.6/2.4
		Oxidation	860	CO_2	1.0
2	None	Deposition	810	CH_4	2.4
3	940° C anneal for 1 h	Oxidation	860	AGR	41.4
	None	Oxidation	950	AGR	41.4

contained in thin silica buckets [8] to catch spalled material. The buckets were removed periodically for weighing. In the oxidation tests only, the spalled oxide was weighed separately and not returned to the specimen bucket on the assumption that it consisted solely of unreactive oxide.

Some specimens were annealed prior to the tests. For carbon deposition experiments, specimens were used either 'as-prepared' or after vacuum annealing (2×10^{-2} Torr) for 50 h at 1100° C. The latter is comparable, although more severe, than the annealing which normally occurs during pack-diffusion treatments. Specimens used in the high-pressure oxidation tests at 860° C were vacuum annealed for 1 h at 940° C, which is equivalent to the maximum temperature–time of heat treatment during manufacture of the fuel cans. It helps to remove stresses and may improve adhesion by allowing a limited interdiffusion which would reduce the sharp compositional discontinuity at the fuel clad–coating interface. Prior heat treatment was not used for specimens reacted at 950° C as the exposure times and the temperature exceeds the standard factory annealing conditions.

Other materials used in the tests include uncoated, factory hydrogen-annealed AGR fuel cladding, arc-melted pure chromium, and hard aqueous electrodeposited chromium.

3. Results

3.1. *Carbon deposition*

Carbon uptake curves for chromium-coated samples are compared with uncoated 20/25 niobium steel control specimens in Fig. 2. The uncoated specimens have a weight gain curve typical of the shape expected at the beginning of this autocatalytic reaction [9]. After an exposure

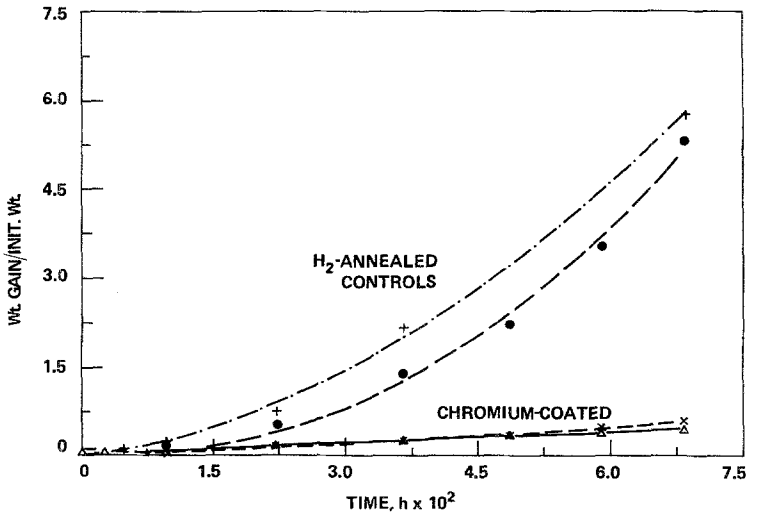

Fig. 2. Carbon deposition on as-prepared electrodeposited chromium-coated and H_2-annealed uncoated 20/25 niobium steel, from methane at 805° C and 2.4 × 10^5 Pa. Carbon uptake expressed as weight gain/initial specimen weight.

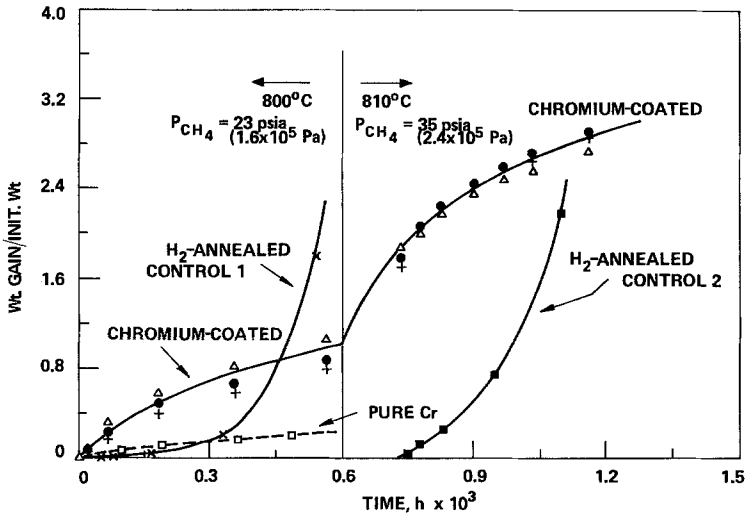

Fig. 3. Carbon deposition from methane on chromium-coated 20/25 niobium steel after vacuum annealing at 1100° C for 50 h, on pure arc-melted chromium and on H_2-annealed uncoated steel control specimens.

to CH_4 for ~640 h, the chromium-coated specimens show a benefit factor of ~ × 11. This compares with benefit factors of ~ × 12.5 for 25 μm and ~ × 32 for 50 μm pack-diffusion chromized samples for the same reaction time under identical reaction conditions [2].

Specimens annealed for 50 h at 1100° C initially take up carbon more rapidly than the untreated alloy (Fig. 3) because of iron made available at the surface by interdiffusion. The weight-gain curve is not typical of an autocatalytic reaction because the rate falls as the small amount of available iron is used up or deactivated. Increasing the severity of the deposition conditions by raising the methane pressure by 42% results in a faster deposition and earlier disintegration of the new control specimen, but the behaviour of the chromium-coated specimen remains similar, although initially supporting deposition at a higher rate. This initially higher rate after exposure of the specimens to the higher methane pressure can be explained satisfactorily on the solution–precipitation mechanism of carbon deposition. The higher pressure would result in an increased equilibrium uptake of carbon in solution in the metal and consequently formation of additional nucleation sites for carbon precipitation [9, 10].

3.2. *Oxidation*

Oxidation rate data is plotted in Figs 4–9. A

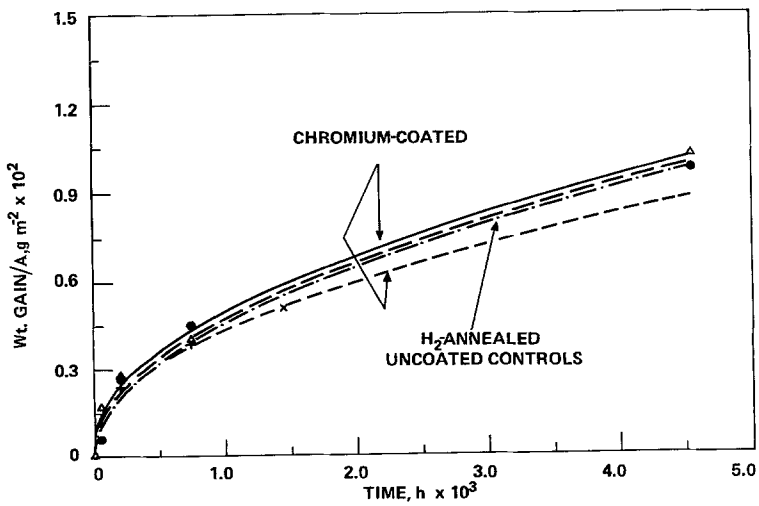

Fig. 4. Weight-gain curves for chromium-coated and uncoated H_2-annealed 20/25 niobium steel oxidized at 950° C in AGR gas at 41 × 10^5 Pa.

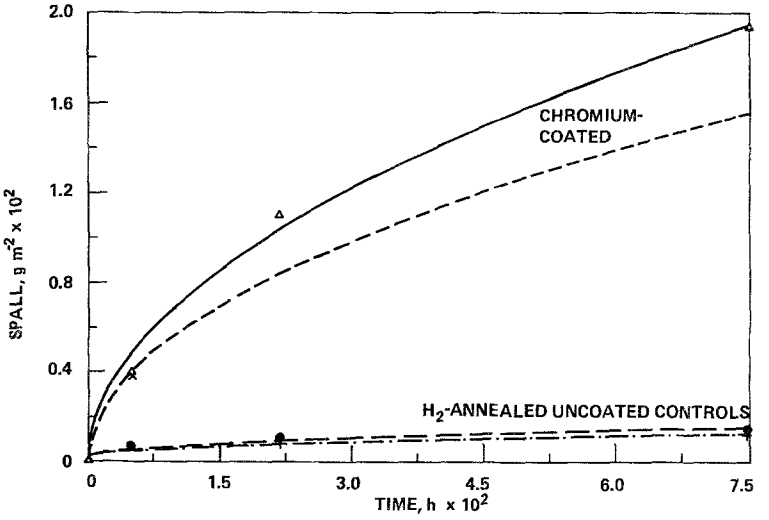

Fig. 5. Oxide spalling curves for chromium-coated and uncoated H_2-annealed 20/25 niobium steel after reaction in 41 × 10^5 Pa AGR gas at 950° C.

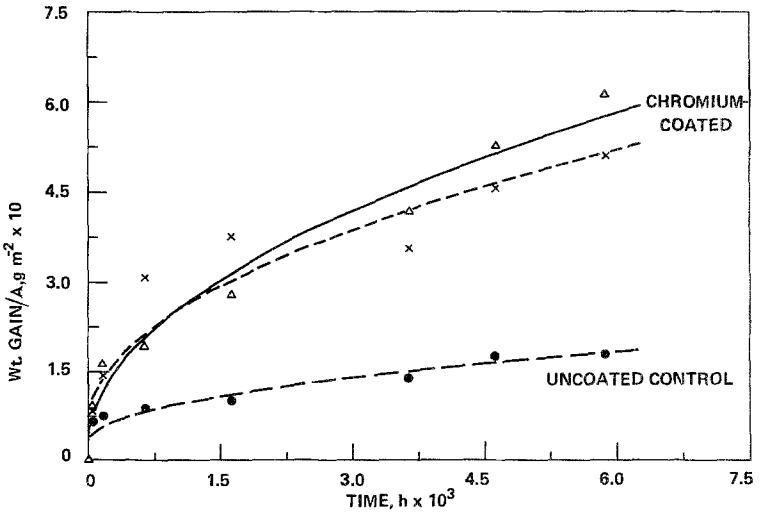

Fig. 6. Oxidation weight-gain curves for chromium-coated and uncoated H_2-annealed 20/25 steel at 860° C and 41 × 10^5 Pa AGR gas.

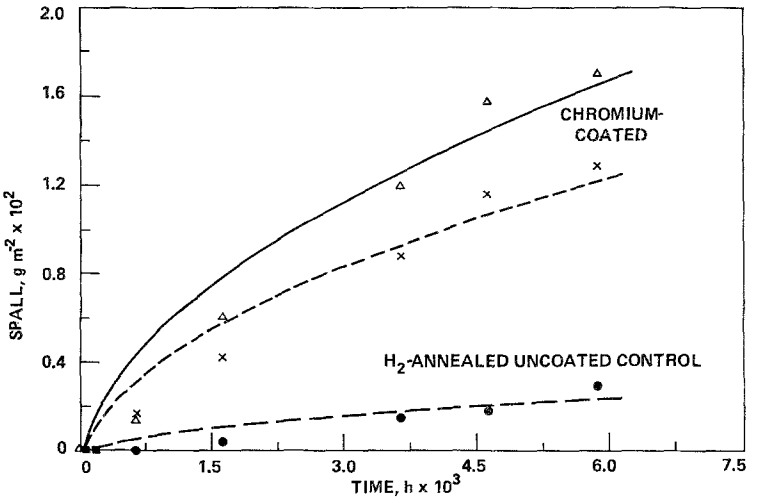

Fig. 7. Spallation during the 860° C high-pressure oxidation, plotted with a parabolic curve fit.

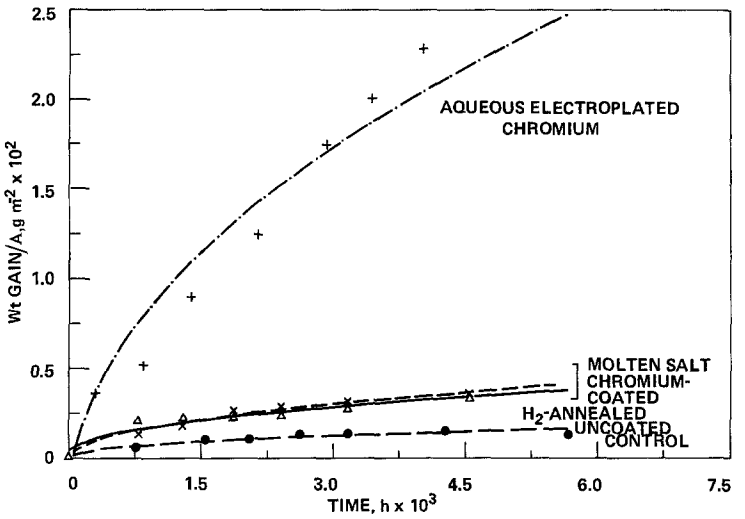

Fig. 8. Weight-gain curves for low pressure oxidation of chromium-coated 20/25 niobium steel, pure aqueous electroplated chromium, and an uncoated control specimen at 860° C in CO_2 gas at 1.0×10^5 Pa.

parabolic curve fits the data for exposures up to the maximum of 6000 h used in the tests. Spalling data is plotted separately and can also be fitted to a parabolic curve. The average rate constants are collected together in Table 3.

At 950° C the coated specimens and uncoated controls appear to oxidize at approximately the same rate (Fig. 4). The spalling from the coated specimen (Fig. 5), however, exceeds that of the controls by a factor of 25 (Table 3). It is possible that the coating has spalled to such an extent that the majority of the reaction is occurring on the unprotected alloy and therefore oxidizes at the same rate as the uncoated material. Because the spall is not returned to the autoclave, oxidation of spalled chromium does not contribute to the measured gross oxidation weight gain. Fig. 5 shows that spalling of the coated specimen occurs continuously throughout the 4500 h of oxidation and is greater than that of the uncoated specimens; therefore, coating must be present on the surface throughout. The results suggest that the oxidation of pure chromium and 20/25 niobium steel may be similar at 950° C.

The chromium-coated specimens oxidize approximately 3 times faster than the uncoated controls at 860° C (Figs 6, 8 and Table 3). At 41×10^5 Pa, the oxide spalling from the coated specimen is 5.6 times that from the uncoated control (Fig. 7). When the metal is undergoing protective diffusion-controlled oxidation with parabolic kinetics, the spalling is expected to follow a similar average rate curve.

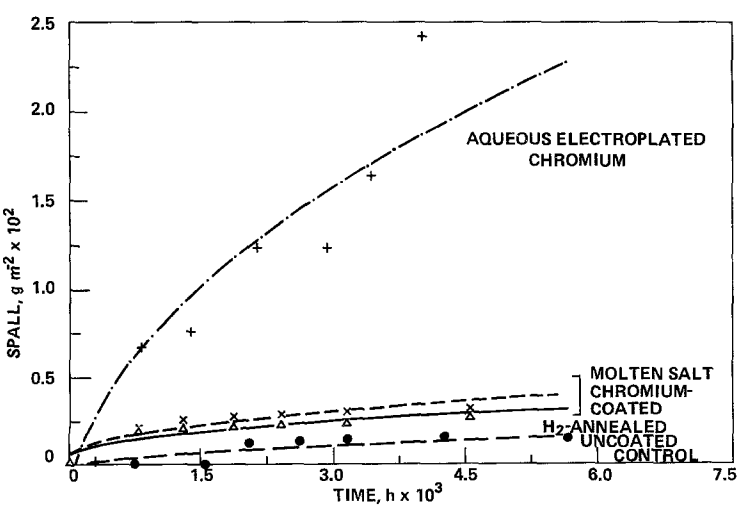

Fig. 9. Spall weight versus time curves for oxidation at 860° C in CO_2 gas at 1.0×10^5 Pa.

Table 3. Average rate constants for CO_2 oxidation

Oxidation conditions				$W = a + bt^{1/2}$		*Relative oxidation rates*	$s = a^1 + b^1t^{1/2}$		*Ratio of spall rates*
Material	*Gas*	*Temperature (° C)*	*Pressure (Pa × 10^5)*	*a*	*b*		a^1	b^1	
Chromium coating	AGR	950	41.4	2.73	1.38	0.9	−6.70	7.40	25.2
Control				−0.46	1.48	1	5.10	0.29	1
Chromium coated	AGR	860	41.4	4.32	0.658	3.3	−0.261	2.25	5.6
Control				3.18	0.198	1	−6.00	0.40	1
Chromium coated				1.29	0.519	2.4	14.71	0.22	0.6
Aqueous electro-deposited chromium	CO_2	860	1.0	−0.27	3.65	17.1	−75.60	4.34	11.4
Control				0.95	0.213	1	−0.10	0.38	1

W = Gross weight gain; s = spall weight; a and a^1, $g\,m^{-2}$; b and b^1, $g\,m^{-2}\,h^{-1/2}$.

In the low pressure oxidation tests, the coated material oxidizes 2.4 times faster than the uncoated alloy. An aqueous electrodeposited pure chromium specimen, however, reacts 17 times faster than the control (Fig. 8). The initial spall, at the end of the first autoclave temperature cycle, is greater on the coated specimen than the control, but thereafter the spall rate is only about half that of the control (Fig. 9). Consistent with the high oxidation rate, the aqueous electrodeposited chromium spalls 11 times faster than the control.

SEM examination of the coating surface after 50 h exposure at 860° C shows areas of pitting due to spallation (Fig. 10a). In a spalled area on a rib top (Fig. 10b) there is evidence in the light areas of coating loss down to the substrate metal, as confirmed by the iron K_α X-ray map (Fig. 10c).

The oxide growth is accompanied by sintering, as the well-defined chromium crystallites (Fig. 1c) develop a rounded appearance (Fig. 11a) after only 166 h exposure in the oxidizing gas. Three different oxide morphologies co-exist on the surface at 860° C (Fig. 11), i.e. the thin adherent protective film (Fig. 11a), scale-like material (Fig. 11b) which may be a precursor to spalling, and isolated areas of whisker-type growths (Fig. 11c). Very similar morphologies are achieved after reaction at 950° C, with oxide particles of 2–6 μm and whiskers of 0.2–2 μm diameter being formed.

3.3. *Microhardness measurements*

The microhardness of the coating in the 'as-prepared' condition lies in the range 150 to 270 $kg\,mm^{-2}$ measured with a 50 g load (Fig. 12). It is softer than a pure arc-melted chromium (~300 $kg\,mm^{-2}$) which should be free of inter-

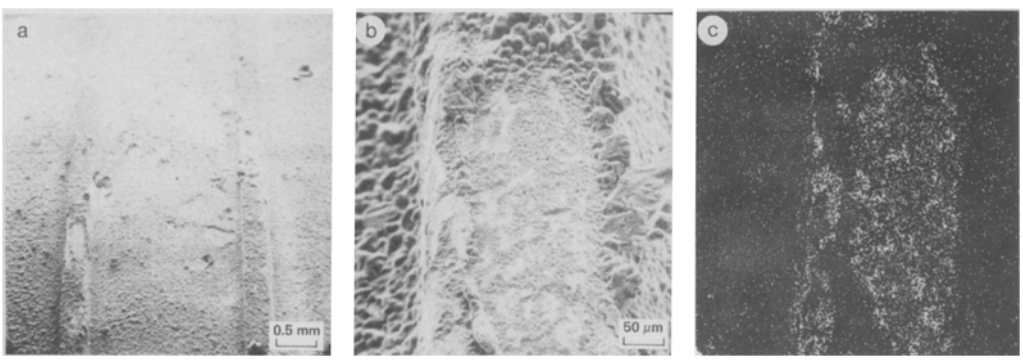

Fig. 10. Oxidized chromium coating after exposure to 41 × 10^5 Pa AGR gas at 860° C for 50 h showing (a) sites of localized spalling; (b) coating spalled to the substrate; (c) iron K_α X-ray map of the area in (b).

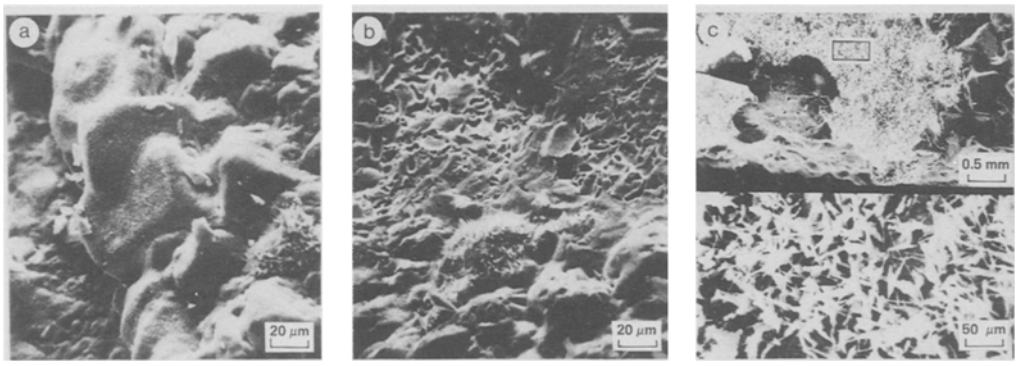

Fig. 11. Oxide morphologies on chromium-coated steel. (a) Thin, adherent oxide layer; (b) scale-like material; (c) whisker growths. Oxidation for 166 h at 860° C in AGR gas at 41 × 10^5 Pa.

stitial and substitutional impurities that could contribute to enhanced hardness. By contrast the aqueous electrodeposited chromium used in the oxidation tests has a microhardness of 1300 kg mm^{-2} and is fairly typical of aqueous electroplated chromium layers.

The hardness of chromium coatings on steels depends on the carbon content of the steel [11]. For example, coatings on cast iron can have values approaching 2000 kg mm^{-2} whereas for low carbon steels (e.g. 0.1% C) the hardness is nearer to 1000 kg mm^{-2}. Both dissolved and precipitated carbon – the latter as dispersed carbide precipitates – can contribute to increased hardness. To check whether the hardness of the molten salt electrodeposited coatings could be increased by carburization, a specimen was exposed to methane at 2.4 × 10^5 Pa for 104 h at 810° C. The treatment time was arbitrarily selected and was merely a first trial condition. From Fig. 12 it can be seen that an approximate increase of 50 kg mm^{-2} in microhardness has been achieved, without any other deleterious change in the specimen. There is obviously scope for the carburizing treatment to increase the hardness further, offering the possibility of tailoring the coating hardness to meet particular requirements, an aspect that is not possible with harder deposits, e.g. aqueous formed coatings. In Fig. 12 the carbon is taken up into solution and has increased the coating hardness over the full 30 μm depth.

The apparently linear hardness relation in Fig. 12 may be a consequence of few experimental points. The substrate hardness of 375 kg mm^{-2} could well be maintained to the

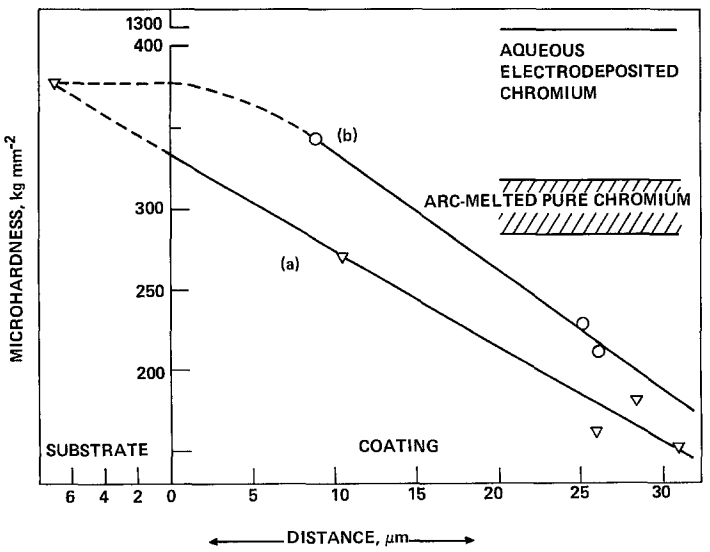

Fig. 12. Knoop microhardness measurements of coating and substrate: (a) as-prepared coating; (b) after exposure to 2.4 × 10^5 Pa methane at 810° C for 104 h.

surface. Also, the correct line (a) in Fig. 12 would lie parallel to line (b). This would imply that solution hardening with carbon would have the same incremental effect throughout the thickness of the coating, and is more readily understood than the situation shown in Fig. 12 where the influence of carbon on hardening is greater nearer the substrate. Local variations in hardness put effective 'error' limits on the experimental points which would permit the two lines to be parallel. Some indication of the variations in hardness over an apparently homogeneous sample are given by the band of values for the arc-melted pure chromium. The overall linear variation in hardness is assumed to be a consequence of the coating technique in which small nuclei are deposited first, followed by the development of larger crystallites.

4. Discussion

4.1. *Carbon deposition protection*

Chromium has a high affinity for carbon and will dissolve it readily at the temperatures of the deposition experiments. After the saturation solubility of carbon in chromium is exceeded, the carbides $Cr_{23}C_6$, Cr_7C_3 and Cr_3C_2 are precipitated successively with increasing carbon content. These carbides are stable to approximately 1500° C. By contrast, the iron carbides are unstable at the temperatures of the deposition experiments. Fe_3C is believed to exist at 800° C [12], but it is likely to be a labile molecule, its stability affected by the local carbon potential. It was suggested previously that the formation and decomposition of labile carbides could account for some of the different morphologies observed in carbon deposits [9]. The chromium carbides have considerable solid solubility for iron, forming the mixed carbides $(Cr, Fe)_{23}C_6$, $(CrFe)_7C_3$ and $(Fe, Cr)_3C$. The effect of combining iron in a stable carbide would reduce its availability to serve as a catalytic intermediate in deposition. Thus, chromium could deactivate the iron catalyst present in the fuel can alloy and thus suppress deposition. On this basis, the mass of chromium in the coating would be more important than the physical structure. This view is consistent with the observation that highly defective pack-diffusion coatings as well as these well crystallized and very pure chromium coats give very similar protection for the same nominal coating thickness.

A simpler view of the deposition protection is that dissolution of carbon in the chromium coating, which takes place initially, lengthens the induction period to deposition and postpones the physical breakdown of the metal surface structure, i.e. the principal mechanism by which most of the catalytic metals are transferred to the growing carbon deposit.

4.2. *Oxidation performance*

The results demonstrate that the coatings do not offer corrosion protection at 860° C and above. At 950° C the coating itself has spalled and it is clear that diffusion bonding would be desirable to improve adhesion. This could be achieved by higher temperature processing, or modifying the electrodeposition process so as to initially plate a mixture of substrate metal and coating metal, changing over to pure coating metal as the deposit grows.

A poor high-temperature oxidation performance could be expected as it is known that Cr_2O_3 scales spall from a chromium surface. The better behaviour of the uncoated alloy in this respect is attributable to the mixed spinel oxide layer formed. After spallation there may be sufficient chromium remaining to allow formation of a healing layer and thus prevent pitting attack.

The low pressure 860° C oxidation performance in CO_2 is better than the high pressure oxidation and spalling in AGR gas. Two factors are different in these tests. The low pressure specimens contained a small quantity of iron in the coating because of the annealing, and would have some diffusion bonding. However, in the high pressure gas the carbon deposition potential was higher and therefore the carbon uptake in the coating would have been greater. Separating the various effects is not possible at this stage.

It was not originally expected that the coatings would be required to give protection at such high temperatures, and indeed they may well provide adequate corrosion behaviour at, say, 700 to 750° C. This is the temperature range at

which carbon deposition is most significant in the nuclear reactor. Furthermore, Cr_2O_3 formed in the oxidation is a good carbon gasification catalyst and could additionally help in suppressing carbon deposition.

The coating oxidation performance is very much better than the aqueous electrodeposited pure bulk chromium. Aqueous electroplates would also be expected to behave poorly at high temperatures, having significant porosity and poor adhesion.

4.3. *Mechanical properties*

The low hardness of the coating may be an advantage in some applications. A soft, ductile coating could be surface finished by mechanical polishing and also deformed to some desired shape after coating, which is impossible with most hard chrome coatings unless a metal such as iron or nickel are incorporated.

The possibility of increasing the hardness to any desired level by a process such as carburization offers interesting possibilities only available with this soft chromium coating. It would be worth exploring further using higher temperatures to permit shorter treatment times, and also considering the alternative hardening technique of nitriding.

4.4. *Optimum coating thickness*

Three factors need to be considered in order to estimate the required minimum coating thickness for this application, i.e.

(i) interdiffusion of iron from the alloy to the coating surface,

(ii) loss of coating by inward diffusion into the bulk alloy,

(iii) conversion of the coating metal to oxide.

The published diffusion data for iron in chromium [13] gives a diffusivity of $1.8 \times 10^{-16}\,cm^2\,s^{-1}$ at 850° C. If a delay to the onset of significant carbon deposition of 2 years is adequate to achieve the required performance of the fuel cladding alloy, then the thickness of chromium required to ensure a surface level of iron not more than 1/100 of the bulk level over this period is $\sim 4.5\,\mu m$. A more demanding situation for this application would be to ensure that the surface iron concentration did not exceed 1/1000 of the bulk level over 7 years (i.e. < 0.055 at % iron at the surface): a chromium coating thickness of $11\,\mu m$ is required to achieve this. The $30\,\mu m$ coating thickness is more than adequate on this basis.

Chromium loss by inward diffusion has been estimated using data published for the lattice diffusion of chromium in fine-grained 20/25 niobium steel [14]. The diffusivity at 850° C is $8.1 \times 10^{-13}\,cm^2\,s^{-1}$ and, using a 'semi-infinite' solid approximation, the chromium concentration at the opposite, uncoated side of the fuel cladding steel would rise by 0.2% in 2 years, and 7% in 5 years. Obviously, loss of protection by diffusion into the bulk alloy is not significant over the required lifetime.

The oxidation performance is the biggest fac-

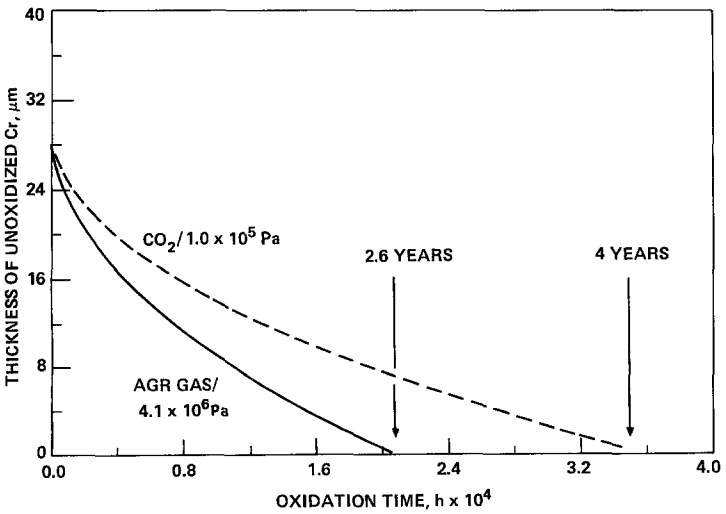

Fig. 13. Conversion of chromium coating to oxide at 860° C, expressed as a loss of coating thickness.

tor influencing the optimum coating thickness. Using the rate data from Table 3, the thickness of the unoxidized metal layer, remaining as a function of oxidation time, has been calculated. It is assumed that the theoretical density of chromium metal is applicable. At 860° C in high pressure AGR gas it is found that the 30 μm coating has a lifetime of 2.6 years, assuming that the parabolic rate law applies throughout this period (Fig. 13). The coating therefore meets the minimum requirement, as discussed above. At 860° C and low pressures the coating has a lifetime of 4 years. The difference reflects the slightly lower oxidation rate at low pressures. The lifetimes shown in Fig. 13 are pessimistic. Any oxide remaining adherent will provide protection against carbon deposition.

There is scope for further improvement in the coatings by some high temperature annealing and, of course, the lifetime could be extended by using a thicker coating.

Acknowledgements

This work was carried out at the Central Electricity Research Laboratories and the paper is published by permission of the Central Electricity Generating Board.

References

[1] A. M. Emsley and M. P. Hill, 16th American Biennial Carbon Conference, American Carbon Society (1983) 192.
[2] *Idem*, 16th American Biennial Carbon Conference, American Carbon Society (1983) 194.
[3] N. C. Cook, Proc. International Conference 'Protection Against Corrosion by Metal Finishing' Basel (1966) 151.
[4] *Idem*, US Patent No. 3 024 177.
[5] M. P. Hill, D. Inman and T. Vargas, UK Patent Application No. GB2, 134545A.
[6] T. Vargas and D. Inman, *J. Appl. Electrochem.* **17** (1987) 270.
[7] A. M. Emsley, M. P. Hill and B. W. Vine, *J. Phys. E., Sci. Instrum.* **13** (1980) 724.
[8] A. M. Emsley, M. P. Hill and P. E. Madden, *ibid.* **13** (1980) 282.
[9] A. M. Brown, A. M. Emsley and M. P. Hill in 'Gas Chemistry in Nuclear Reactors and Large Industrial Plant', Proc. Conf. University of Salford, April 1980, Heydon, London (1980) p. 26.
[10] A. M. Brown and M. P. Hill in 'Coke Formation on Metal Surfaces' American Chemical Society Symposium Series No. 202 (1982) chap. 10.
[11] P. Galmiche, *Rev. Metall.* **47** (1950) 192.
[12] H. J. Goldschmidt, 'Interstitial Alloys', Butterworths, London (1967).
[13] H. W. Paxton and R. A. Wolfe, *Trans. AIME* **230** (1964) 1426.
[14] A. F. Smith and G. B. Gibbs, *Metal Sci. J.* **3** (1969) 93.